# Resonance Charge Transfer and Population Inversion Following $C^{5+}$ and $C^{6+}$ Interactions with Carbon Atoms in a Laser-Generated Plasma*

R. H. Dixon and R. C. Elton
*Naval Research Laboratory, Washington, D. C. 20375*
(Received 2 March 1977)

Enhanced population of the $n=4$ excited state is measured in both $C^{4+}$ and $C^{5+}$ ions in agreement with a theory for formation by resonance charge transfer between carbon ions and atoms. A background gas modifies and mixes the interacting particles originating from a carbon surface vaporized by a focused laser beam. Population inversions capable of producing quasi-cw amplification in the extreme ultraviolet region are measured.

The total cross section for the direct transfer of a bound electron from an atom to a nearby ion can be very large ($\sim 10^{-15}$ cm$^2$ for light elements) under certain conditions. These conditions can occur in the exothermic resonance charge-transfer reaction. Velocity-dependent resonances occur in the cross section and specific bound states of the product ion are selectively populated, leading to possible population inversions.[1] In this Letter we report the first experimental verification of such preferentially populated states in a highly stripped plasma ion at measured velocities in agreement with theory. For this, the required ion-atom interaction region and interval have been defined. This effort has also resulted in the first experimental evidence of quasi-cw population inversion between product-ion energy levels separated by at least 16 eV, appropriate for lasing at wavelengths shorter than 800 Å.

In the resonance charge-transfer process[2] observed, neutral carbon upon collision with a $C^{5+}$ or $C^{6+}$ ion transfers an electron directly into the $n=4$ excited state of the product ion $[(C^{4+})^*$ or $(C^{5+})^*$, respectively], i.e.,

$$C + C^{5+,6+} \rightarrow C^+ + (C^{4+,5+})^* + \Delta E_{i,f}\,. \qquad (1)$$

The energy levels[3,4] involved are shown in Fig. 1. The energy $\Delta E_{i,f}$ is the difference in binding energies of the initial and final states at infinite separation and is in an inverse relationship with a pseudo potential-curve crossing distance, according to the Landau-Zener theory of charge exchange.[2] A reaction is most probable for relative ion-atom velocities which correspond to the crossing point, leading to predicted resonances for the reaction cross section as a function of relative velocities. Sharp resonances with large peak cross sections are predicted at low relative velocities, usually with energy defects in the 10–20 eV range.[2,5] For the reactions reported here, it can be seen from Fig. 1 that this corresponds to the $n=4$ excited product-ion states. The cross-section resonance for $n=4$ state population occurs at velocities as low as $1\times 10^6$ and $8\times 10^6$ cm/sec for the $(C, C^{5+})$ and $(C, C^{6+})$ reactions, respectively. Such velocities are reported below for the present experiment. Direct population of the $n=3$ state requires velocities $> 10^8$ cm/sec. Likewise, $n \geq 5$ state population requires velocities $< 10^6$ cm/sec with very narrow resonances at correspondingly large pseudo crossing distances.

In this experiment[6,7] a 5-J, 16-ns pulse from a Nd:glass laser is focused onto the surface of a carbon slab to a diameter of 0.5 mm by a 200-mm-focal-length lens to produce a target irradiance of $2\times 10^{11}$ W/cm$^2$. An important and novel aspect of this experiment is the addition of a gas-

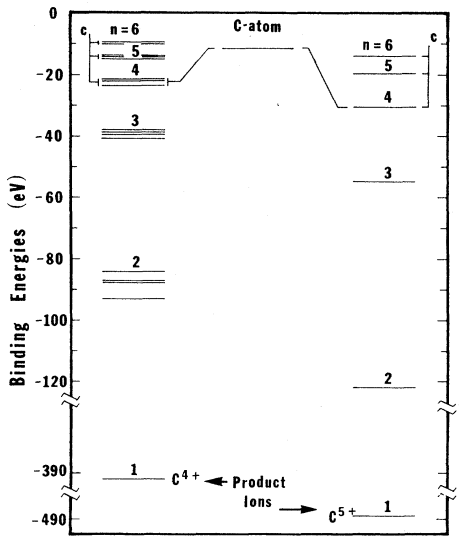


FIG. 1. Binding-energy diagram for an electron in the initial carbon atom and either a $C^{4+}$ or $C^{5+}$ final (product) ion. Electron collisional mixing of the states for $n \geq 4$ is indicated by "$c$." Several potentially mixed (collisionally) levels are indicated for $C^{4+}$.

eous atmosphere which contributes both to the formation of neutral carbon atoms from fast ions and to the attenuation of the expansion velocity of reacting ions. This results in the creation of a vital ion-atom mixing layer 15–25 mm from the target in which appropriate relative velocities exist. The results are generally independent of gas (helium, hydrogen, neon, argon) or pressure (1–10 Torr) used; helium at 1 Torr was chosen for these data, resulting in a relatively uncluttered and useful spectrum for plasma analysis. This independence of the results on gas or pressure disassociated the background atoms as a major reactant [in fact, the energy defects for helium (−24.6-eV binding energy) are appropriate to populating $n=3$ states in the carbon ions (Fig. 1) and not $n=4$ as observed]. At the low pressure chosen, no significant absorption of emitted resonance radiation over a 3-cm path was noticed.

The relative populations of the $n=4$ states in the $C^{4+}$ and $C^{5+}$ product ions were determined mainly from observations of the $np\ ^1P_1 \rightarrow 1s\ ^1S_0$ resonance series spectral lines in the 0–40 Å region as shown in Fig. 2. Spectral dispersion was obtained with a 2.2-m grazing-incidence vacuum spectrograph and spatial resolution along the expansion axis perpendicular to the carbon target was obtained by alignment of the entrance slit with this axis and then inserting a 0.4-mm-wide slot behind and orthogonal to the slit. Exposure of Kodak SWR plates through the "pinhole" formed required typically 180 shots, between each of which the carbon disk target was rotated to a new position. The microdensitometer tracing in Fig. 3 was taken at an optimum distance of 16 mm from the target surface.

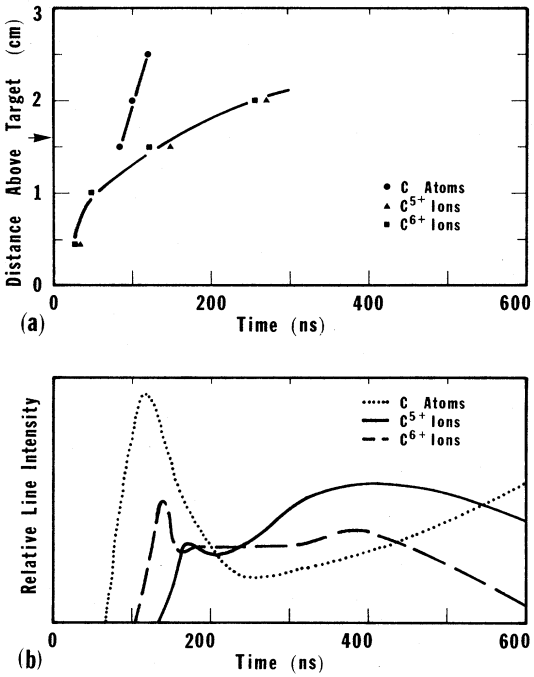


FIG. 2. Temporal behavior of (a) particle trajectories, and (b) relative line intensities (at 3434, 4945, 2479 Å) measured at a distance of 16 mm, [indicated by arrow in (a)]. Sustained emission in the 15–25 mm region (a) explains a hemispherical halo observed on time-integrated photographs.

In Fig. 3 the microdensitometer tracing of film density versus wavelength shows resonance series lines for $n \geq 4$ which are anomalously large relative to what would be expected for the series beginning with the 2-1 and 3-1 transition lines. (The relative intensities for $n \geq 4$ lines resemble a distribution of enhanced emission beginning with a $n=4$ source state.) Such an emission distribution is also evident in the $nd \rightarrow 2p$ and $np \rightarrow 2s$ series spectra from $C^{4+}$ and $C^{5+}$ ions at longer wavelengths. It is not apparent (nor expected) for a $C^{3+}$ product ion.

An electron density of $\approx 5\times 10^{16}$ cm$^{-3}$ was measured in this plasma region (16 mm from the target surface) from Stark-broadened[8] He II lines at 3203 and 4686 Å. (This density rises with increased fill pressure, indicating at least a partial background gas origin for free electrons.) The collision limit[9] occurring at about $n=4$, can explain the distribution of the $n=4$ population density among higher-lying states (and the continuum) by electron collisional excitation. Charge

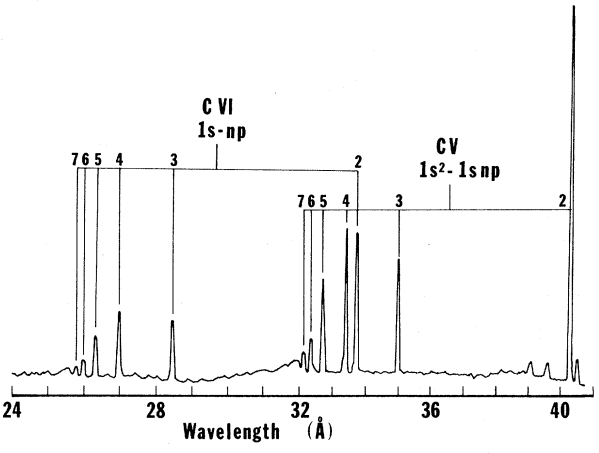


FIG. 3. Micordensitometer tracing at a distance of 16 mm from the target of a second-order time integrated C V ($C^{4+}$ ions) and C VI ($C^{5+}$ ions) spectrum from 180 exposures. True wavelengths are indicated.

transfer directly into $n = 5$ levels cannot be completely ruled out if some ions are slowed sufficiently at late times. The distribution of resonance line emission illustrated in Fig. 3 is consistent with a simple model in which collisionally mixed levels of $n \geq 4$ cascade radiatively to $n = 3$, 2, and 1 levels, so that additional excitation from the ground state or recombination need not be invoked for the interpretation. This is as expected since the high-probability resonance charge-transfer process dominates over all others[9] for a reasonable density of neutrals. Opacity effects[9] are not significant at the ion ground-state densities of $\lesssim 10^{15}$ cm$^{-3}$ expected for the energy deposited by the laser.

Expansion into a vacuum does not produce measurable emission beyond 1 cm from the target.[7,11] Within this distance, however, there is some evidence of enhanced $n = 3$ emission on time-integrated spectra. It is known that vaporized neutral carbon may expand slowly ($v \sim 10^5$ cm/sec) from the surface[12] and some interaction with ions is indeed possible, although not as reliably nor as conveniently for analysis as in the more distant zone created with a gaseous background.

The plasma/gas plume was first photographed in visible light with and without temporal resolution and showed a luminous shell of plasma 10–25 mm from the surface, formed approximately 100 ns after laser irradiation and unique to the gas-filled experiment. The time histories of the $C^{6+}$, $C^{5+}$, $C^{4+}$, and $C^{+}$ ions and the neutral carbon atoms were determined from photoelectric measurements using a 0.5-m Czerny-Turner mounted monochromator imaged at discrete distances above the target. The ions monitored, the transitions (subscripts) and the wavelengths are $C^{5+}_{7-6}$ (3434 Å), $C^{4+}_{7-7}$ (4945 Å), $C^{4+}_{2-2}$ (2271 Å), $C^{+}_{4-3}$ (4627 Å), and $C_{3-2}$ (2479 Å) [lines from the higher lying (7-6) transitions correlate with the next-higher ionic species[11]]. Time corresponding to the half-intensity points on the leading edge of the signal for each species are measured from the initial surface-illumination time and are plotted in Fig. 2(a) at various distances. They are connected by a smooth curve that closely follows the luminous front trajectory obtained from streak photographs. A vital phenomenon observed is the early formation of a significant density of neutral carbon atoms in the 15–25 mm region above the target. These atoms are formed by the rapid neutralization of ions initially accelerated from the target. [Similar data taken in a vacuum ($< 10^{-3}$ Torr) environment show highly ionized species following the same early trajectory; see Ref. 11 also.] Momentum transfer during and after recombination apparently leaves the carbon atoms in this region static equilibrium. Also of importance is the observed velocity attenuation for the sheath of ions moving into the preformed atomic atmosphere with velocities appropriate to the charge-transfer reaction.

Of equal importance to the spatial overlap between ions and atoms is the temporal coincidence, particularly when analyzing time-integrated spectra (Fig. 3). The temporal behavior of the atoms and interacting ions at 16 mm is shown in Fig. 2(b), which indicates the continued presence of carbon atoms in the interaction zone and the depletion of these atoms as the ions enter the zone. A mean relative velocity of these entering ions was deduced from Fig. 2(a) and the value of $\sim 5 \times 10^6$ cm/sec is consistent with the theoretical range given above for charge exchange into the $n = 4$ levels. The presence of C signals after $C^{6+}$ and $C^{5+}$ depletion supports a model in which the carbon atoms remain stationary in the interaction zone.

Relative population densities for $n = 5$, 4, and 3 levels in the $C^{4+}$ and $C^{5+}$ product ions were determined from the data of Fig. 3 by converting film density to exposure using a calibration obtained with multiple exposures, and by dividing the relative intensities found by the appropriate transition probabilities for degenerate levels of each quantum number. After dividing by statistical weights $\omega_n$, the relative reduced population densities $N_n/\omega_n$ for $n = 5$, 4, and 3 were found to be in the ratios of 3.8:3.4:1 for $C^{4+}$ and 3.8:2.6:1 for $C^{5+}$, respectively, indicating the definite presence of population inversion for transitions 4-3 and 5-3 of each species. Significant inversion on 5-4 was not expected with collisional mixing; indeed, the ratios between the $n = 5$ and $n = 4$ levels are nearly consistent with collisional excitation of the ions as they move into a stationary electron cloud with the measured velocity. The inversions continue for the duration of the reaction region, i.e., in a quasi-cw state, since the rate of $n = 3$ decay exceeds the population rate. With sufficient density, the potential for amplification of spontaneous emission[13] exists at wavelengths[4] extending from 350–760 Å. However, for the energy deposited here an excited ion density exceeding $\sim 10^{14}$ cm$^{-3}$ cannot be expected 16 mm above the target, with a calculated amplification too small to observe. With the large cross section involved and favorable wavelength scal-

scaling, a density of $10^{16}$ should be sufficient to achieve measurable amplification.[13] Such conditions may be developed closer to the target, with higher gas pressures, with increased laser energy, or with more volatile targets. Also, increased reactions can possibly be generated with synchronized dual laser pulses designed to intentionally inject additional ions from a target after an atomic vapor is formed.

The technical assistance of D. P. Jew and J. L. Ford in obtaining the data is gratefully acknowledged, as are helpful discussions with H. R. Griem, T. N. Lee, and E. A. McLean. Constructive interactions with R. A. Andrews in originally formulating this project are recalled with appreciation.

*Work supported in part by the U. S. Energy Research and Development Administration under Contract No. E(49-20)-1010.

[1]A. V. Vinogradov and I. I. Sobel'man, Zh. Eksp. Teor. Fiz. 63, 2113 (1973) [Sov. Phys. JETP 36, 1115 (1973)].

[2]H. J. Zwally and D. W. Koopman, Phys. Rev. A 2, 1850 (1970); H. J. Zwally, Ph.D. thesis, University of Maryland, 1970 (unpublished).

[3]C. E. Moore, *Atomic Energy Levels*, U. S. National Bureau of Standards, National Standard Reference Data Systems—35 (U.S. G.P.O., Washington, D. C., 1971), Vol. 1.

[4]R. L. Kelly and L. J. Palumbo, Naval Research Laboratory Report No. 7599, 1973 (unpublished).

[5]J. Goldhar, R. Mariella, Jr., and A. Javan, Appl. Phys. Lett. 29, 96 (1976).

[6]R. C. Elton, in *Progress in Lasers and Laser Fusion*, edited by B. Kursunoglu, A. Perlmutter, and S. M. Widmayer (Plenum, New York, 1975).

[7]R. C. Elton and R. H. Dixon, Ann. N. Y. Acad. Sci. 267, 3 (1976); also R. C. Elton and R. H. Dixon, in *Beam Foil Spectroscopy*, edited by I. A. Sellin and D. J. Pegg (Plenum, New York, 1976).

[8]H. R. Griem, *Spectral Lines Broadening by Plasmas* (Academic, New York, 1974).

[9]R. C. Elton, in *Methods of Experimental Physics, Plasma Physics*, edited by H. R. Griem and R. H. Lovberg (Academic, New York, 1970), Vol. 9A, Chap. 4.

[10]W. L. Wiese, M. W. Smith, and B. M. Glennon, *Atomic Transition Probabilities: Hydrogen Through Neon*, U. S. National Bureau of Standards Publication, National Standard Reference Data Systems—4 (U.S. G.P.O., Washington, D. C., 1966), Vol. I.

[11]B. C. Boland, F. E. Irons, and R. W. P. McWhirter, J.Phys. B 1, 1180 (1968).

[12]J. R. Greig and R. E. Pechacek, J. Appl. Phys. 48, 596 (1977).

[13]R. W. Waynant and R. C. Elton, Proc. IEEE 64, 1059 (1976).

# Hartree-Fock Calculations for Atoms with Inner-Shell Vacancies

Charlotte Froese Fischer
*Department of Computer Science, The Pennsylvania State University, University Park, Pennsylvania 16802*
(Received 28 February 1977)

For configuration states such as $2p^5 3p^5\ {}^1S, {}^3P, {}^1D$ the Hartree-Fock method produces total wave functions with an incorrect form as the atomic number $Z \to \infty$. It is shown how a correct form can be obtained, with similar accuracy as the Hartree-Fock wave function, for a statistically weighted average of $2p^5 3p^5\ {}^3S, {}^1P, {}^3D$.

Atomic inner-shell processes usually lead to configurations with several open shells. For some of the associated configuration states, the Hartree-Fock method may yield rather poor results.

Several configurations studied to date have contained subshells $2p^5 3p^5$, all other electrons being $s$ electrons.[1-3] Let us consider the states of $Ar^{+2}$ where all the other subshells are complete. Then the allowed $LS$ term values are ${}^{1,3}S, P, D$. Now the Hartree-Fock approximation is characterized by the fact that the energy is stationary with repect to all allowed perturbations. Let $P_{2p}{}^{\mathrm{HF}}$, $P_{3p}{}^{\mathrm{HF}}$ be Hartree-Fock radial functions and $\Phi^{\mathrm{HF}}$ the Hartree-Fock wave function.

Two types of perturbations may be applied[4,5]: One is

$$P_{2p} = P_{2p}{}^{\mathrm{HF}} + \epsilon P_{np}; \quad \langle P_{2p} | P_{np} \rangle = \langle P_{3p} | P_{np} \rangle = 0.$$

Then

$$\Phi = \Phi^{\mathrm{HF}} + \epsilon \Phi_{2p \to np} + O(\epsilon^2),$$

where it can be shown that $\Phi_{2p \to np}$ is a linear combination of states $2p^4(L'S')np(^2P) \cdot 3p^5 LS$. The second is

$$\begin{bmatrix} P_{2p} \\ P_{3p} \end{bmatrix} = \begin{bmatrix} 1 & -\epsilon \\ \epsilon & 1 \end{bmatrix} \begin{bmatrix} P_{2p}{}^{\mathrm{HF}} \\ P_{3p}{}^{\mathrm{HF}} \end{bmatrix}.$$